Supporting Information

Efficient photooxidation of C(sp^3)-H bonds on visible-light-responsive W-doped TiO_2 nanocrystals promoted by photochromic effect

Zhen Zhang[1], Yun Zhang[1], Chaowei Han, Mei Yan, Guanfeng Ji*, Wenshou Wang*

School of Chemistry and Chemical Engineering, University of Jinan, Jinan 250022, P.R. China

[1] These authors contributed equally to this work.

*Corresponding Authors: chm_jigf@ujn.edu.cn, chm_wangws@ujn.edu.cn

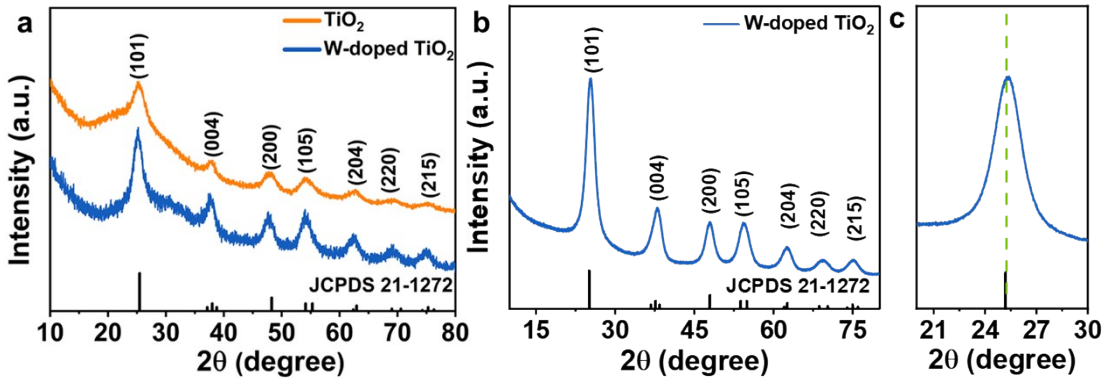

Fig. S1. (a) XRD patterns of TiO_2 and W-doped TiO_2 nanocrystals. (b and c) XRD patterns of various photocatalysts at 2θ of 20−80° (b) and 20−30° (c).

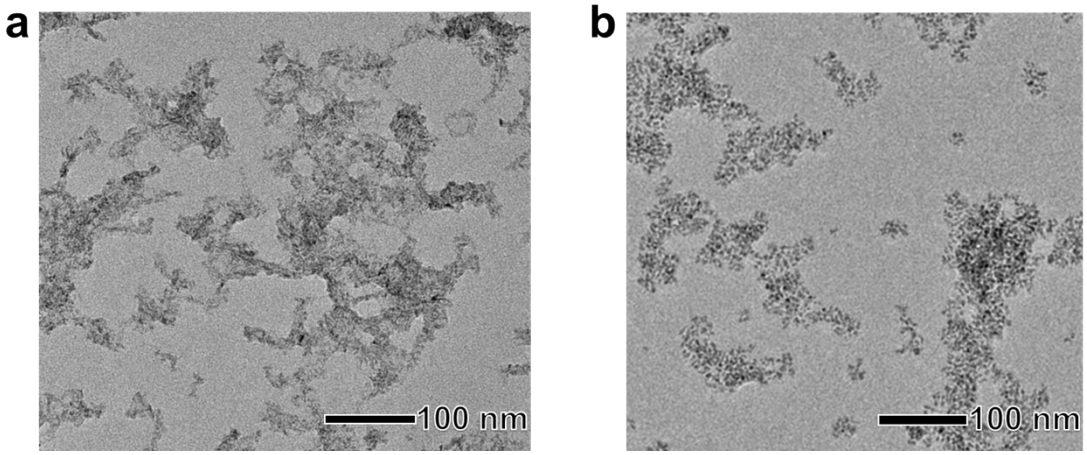

Fig. S2. High-magnification TEM images of (a) TiO_2 and (b) W-doped TiO_2 nanocrystals.

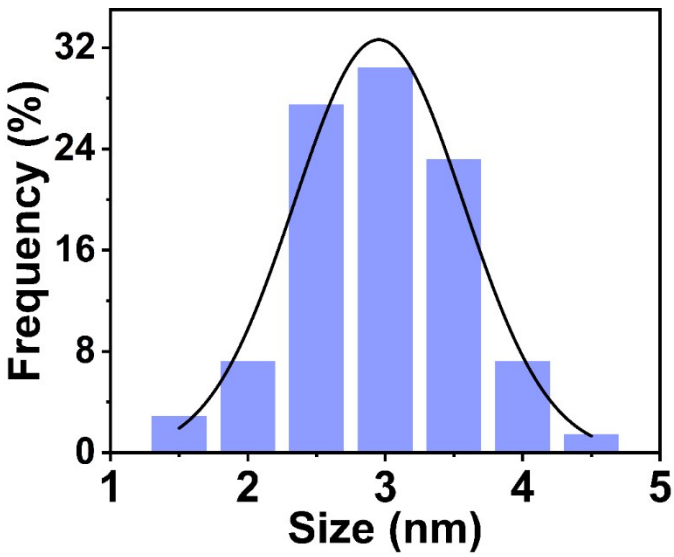

Fig. S3. Size distribution histogram of the W-doped TiO_2 nanocrystals.

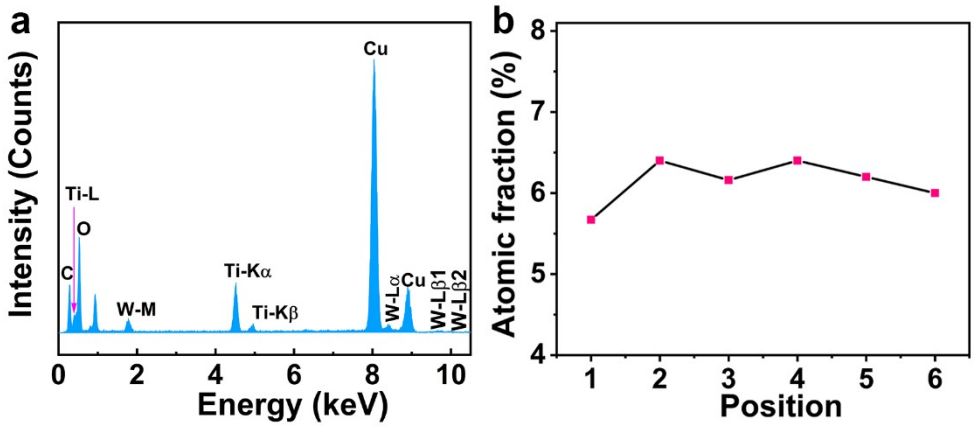

Fig. S4. (a) The energy-dispersive X-ray spectrometry; (b) W/Ti proportion statistics collected from six random W-doped TiO_2 nanocrystals.

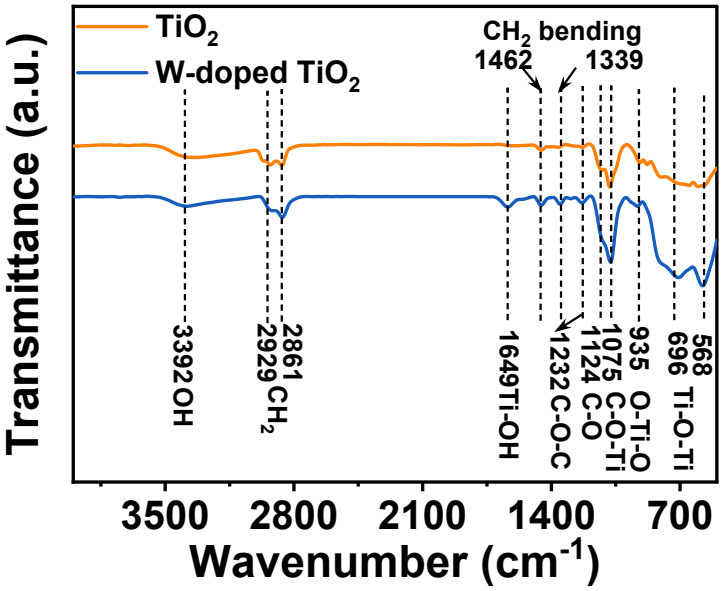

Fig. S5. FT-IR spectra of W-doped TiO_2 and TiO_2 nanocrystals.

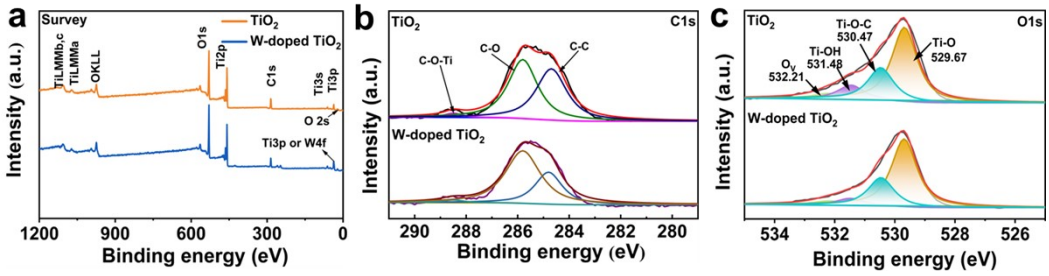

Fig. S6. (a) survey XPS spectra, (b, c) High resolution XPS spectra of C1s (b) and O 1s (c) of TiO_2 and W-doped TiO_2 nanocrystals.

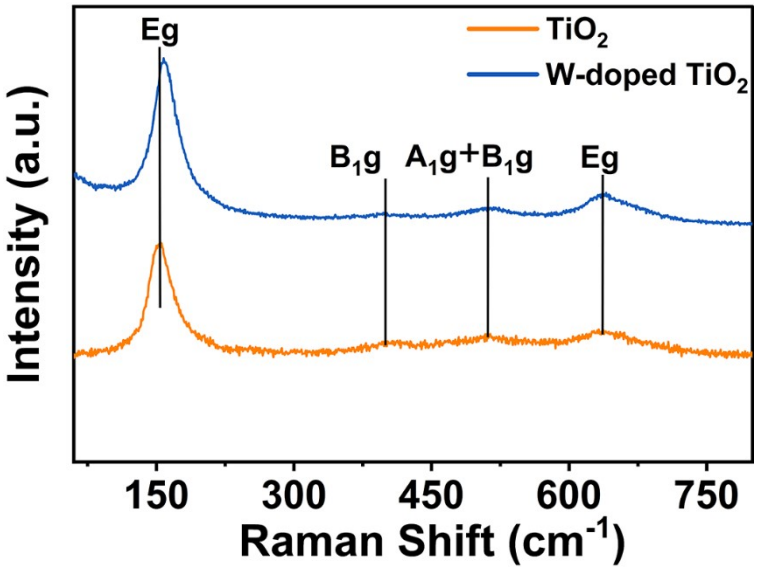

Fig. S7. Raman spectra of TiO_2 and W-doped TiO_2 nanocrystals.

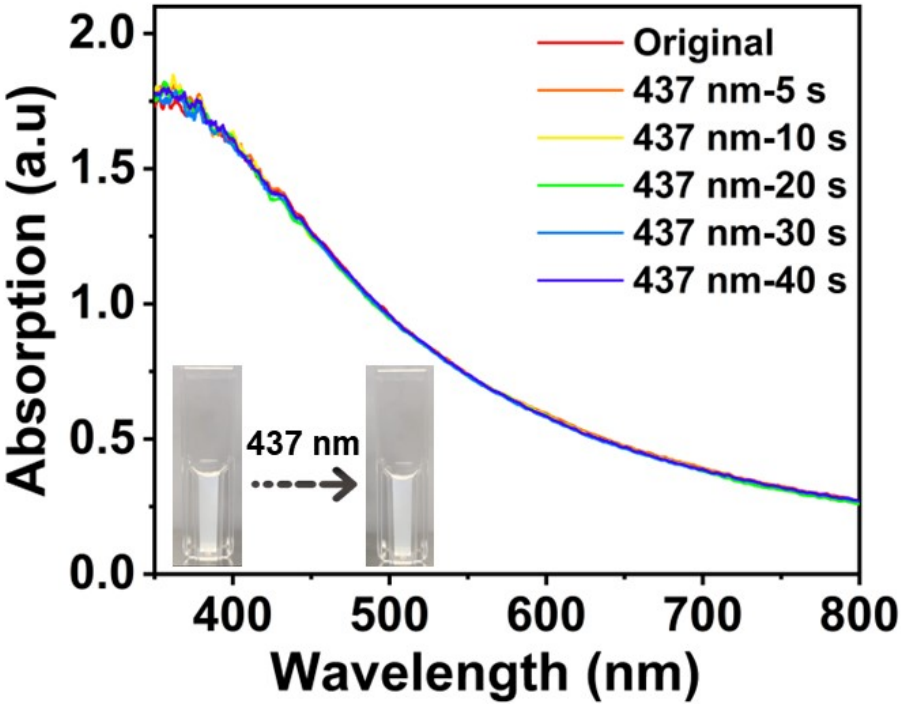

Fig. S8. UV-vis spectra of TiO_2 nanocrystals showing the coloration process upon 437 nm irradiation. Insets are the digital photographs of samples before and after 437 nm irradiation.

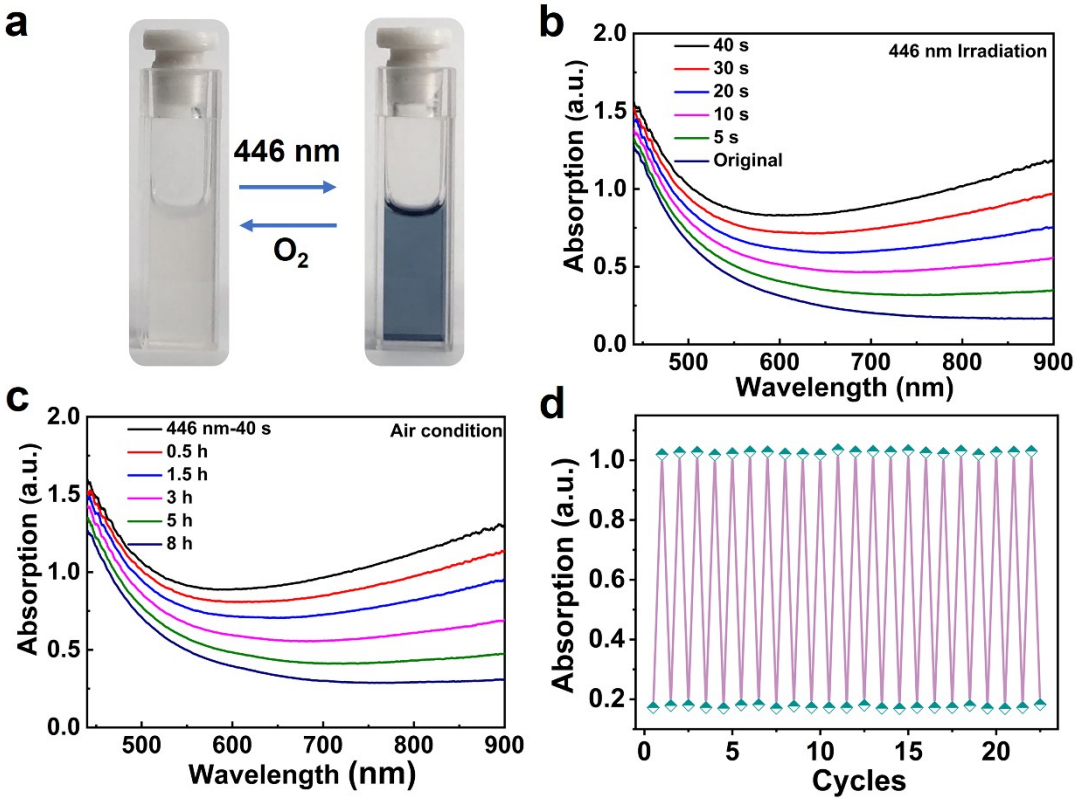

Fig. S9. Photoreversible color switching of the W-doped TiO_2 nanocrystals. (a) Color switching of the aqueous mixture upon 446 nm irradiation. UV-vis spectra showing (b) the coloration process upon 446 nm irradiation, (c) the decoloration process in air. (d) The absorption intensity of the system at 800 nm was recorded for 22 cycles.

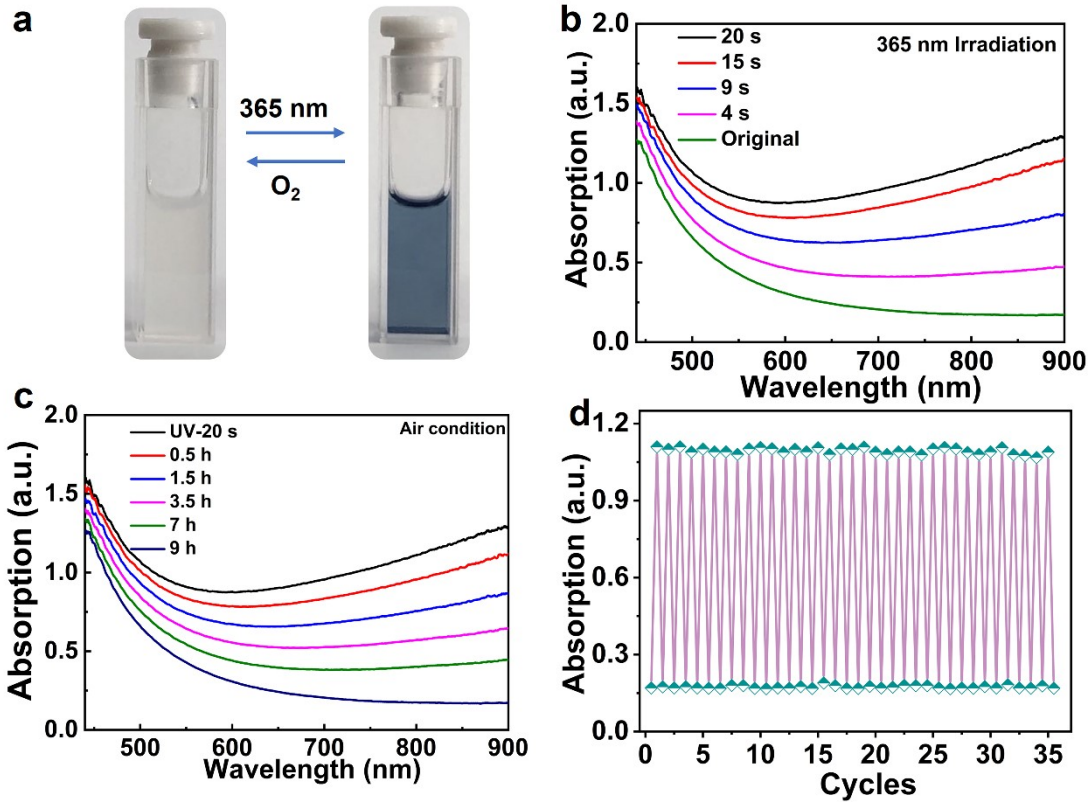

Fig. S10. Photoreversible color switching of the W-doped TiO_2 nanocrystals. (a) Color switching of the aqueous mixture upon 365 nm irradiation. UV-vis spectra showing (b) the coloration process upon 365 nm irradiation, (c) the decoloration process in air. (d) The absorption intensity of the system at 800 nm was recorded for for 35 cycles.

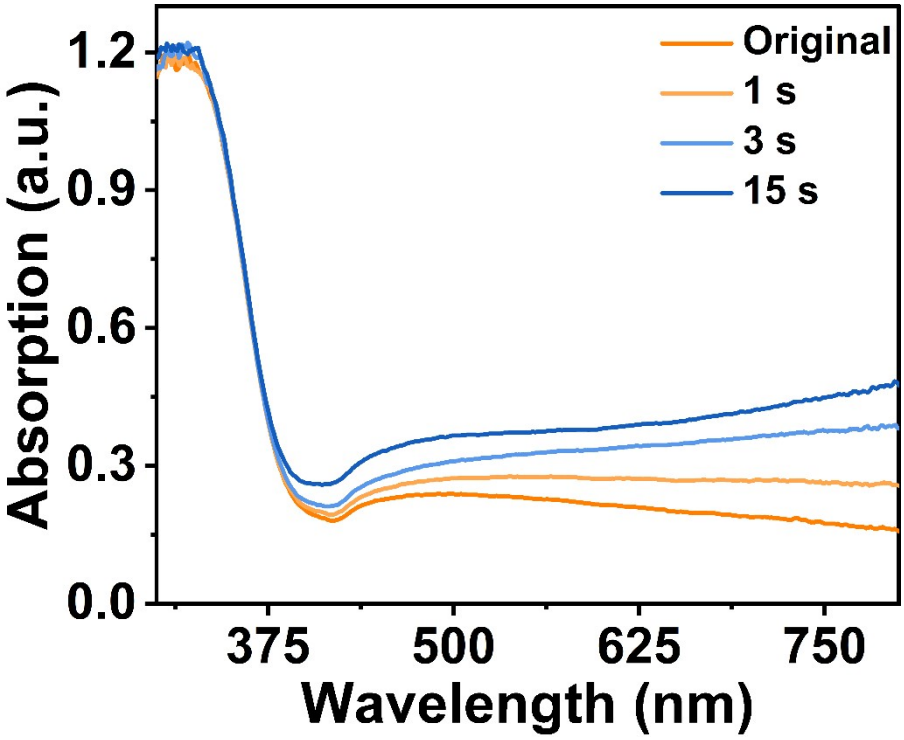

Fig. S11. UV-vis spectra of W-doped TiO_2 nanocrystals of the ethylbenzene/acetonitrile (1:1) solution showing the coloration process upon 437 nm irradiation.

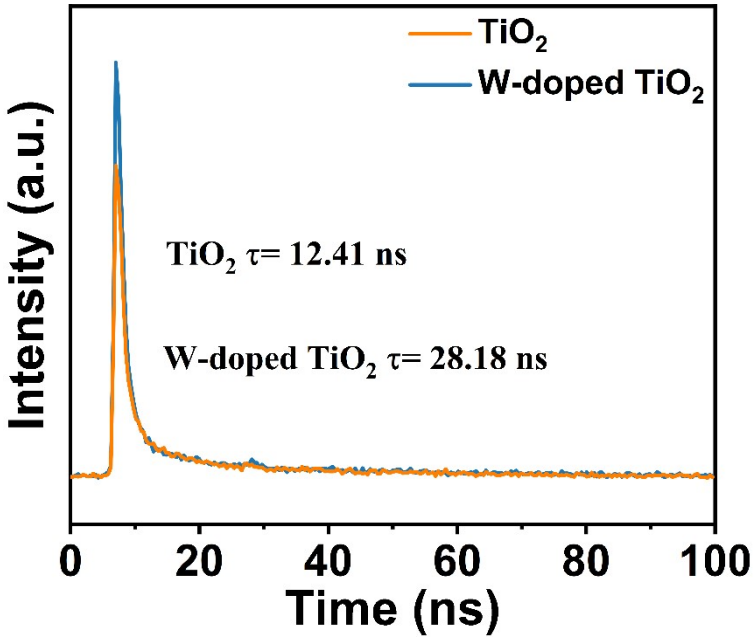

Fig. S12. Time-dependent fluorescence decay traces of TiO_2 nanoparticles and W-doped TiO_2 nanocrystals.

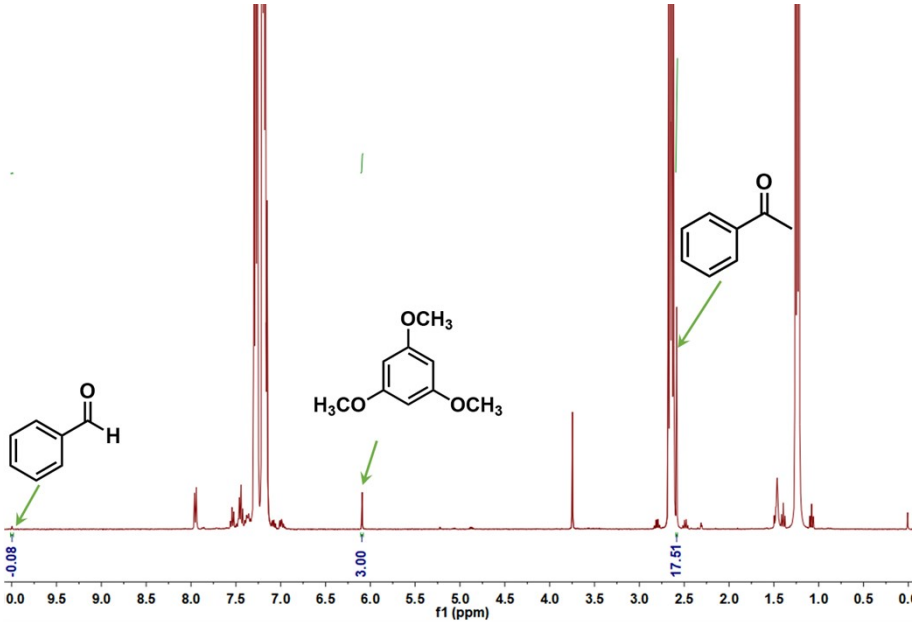

Fig. S13. ^{1}H NMR spectrum for photooxygenation reaction of ethylbenzene. The internal standard peak at 6.09 ppm and the product peak at 2.58 and 10.1 ppm were used to calculate the conversion rates (0.1 mmol 1,3,5-trimethoxybenzene as internal standard).

The apparent quantum yield (AQY) for the conversion of ethylbenzene was measured using a 437 nm monochromatic light. The total illustration was 0.018 W cm^{-2}. The irradiation area was controlled as 13.2 cm^2. Depending on the amount of converted ethylbenzene by the photocatalytic reaction in 6 hours, and the AQY was calculated as follow[1]:

$$AQY = \frac{N_e}{N_p} \times 100\% = \frac{10^9(\nu \times N_A \times K) \times (h \times c)}{(I \times A \times \lambda)} \times 100\% = \frac{1.2 \times 10^8(\nu \times K)}{(I \times A \times \lambda)}$$

Where, N_e represents the number of electrons available for production of acetophenone, N_p represents the number of incident photons, N_A represents Avogadro constant (6.022×10^{23} mol^{-1}), ν is the production rate of acetophenone ($mol\cdot s^{-1}$), $\hbar$ represents the Planck constant (6.626×10^{-34} J·s), c represents the speed of light (3×10^8 m s^{-1}), A represents the irradiation area (m^2), I represents the intensity of irradiation light (W m^{-2}), λ represents the wavelength of the monochromatic light (nm).

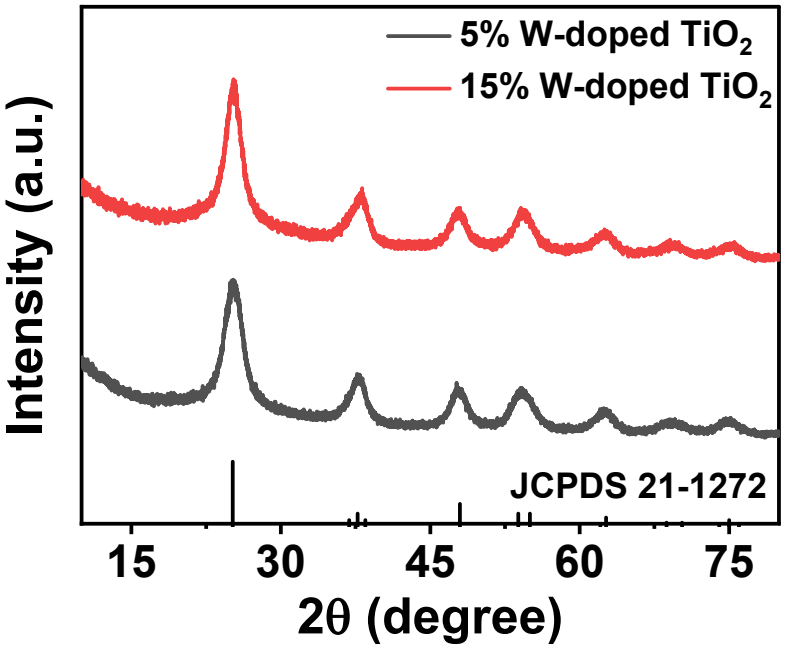

Fig. S14. XRD patterns of 5% and 15% W-doped TiO_2 nanocrystals.

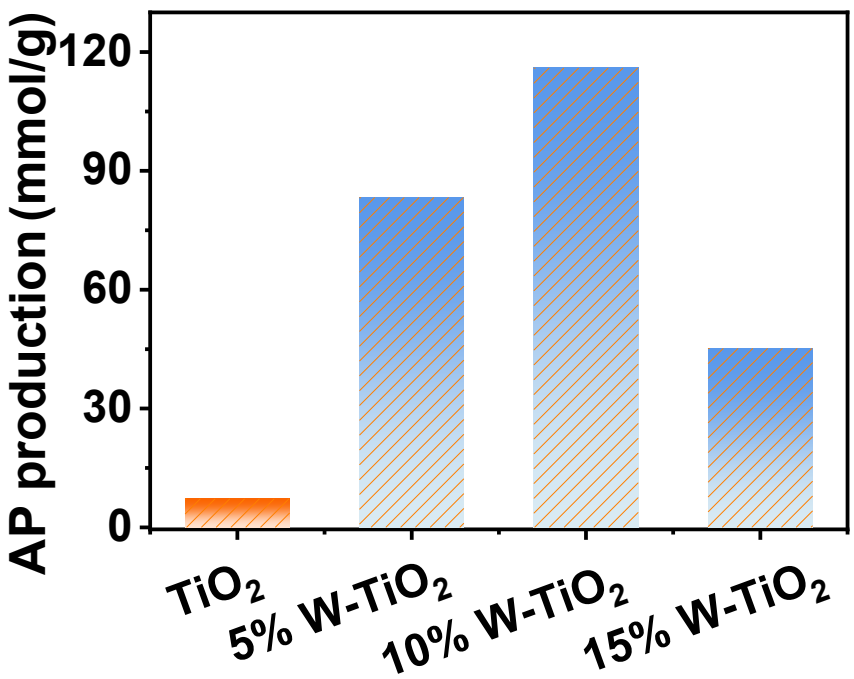

Fig. S15. Histogram of the production of acetophenone (AP) from ethylbenzene over different catalysts. Reaction condition: 298 K, O_2, 3 mL ethylbenzene, 5 mg catalyst, 437 nm light, 6 h.

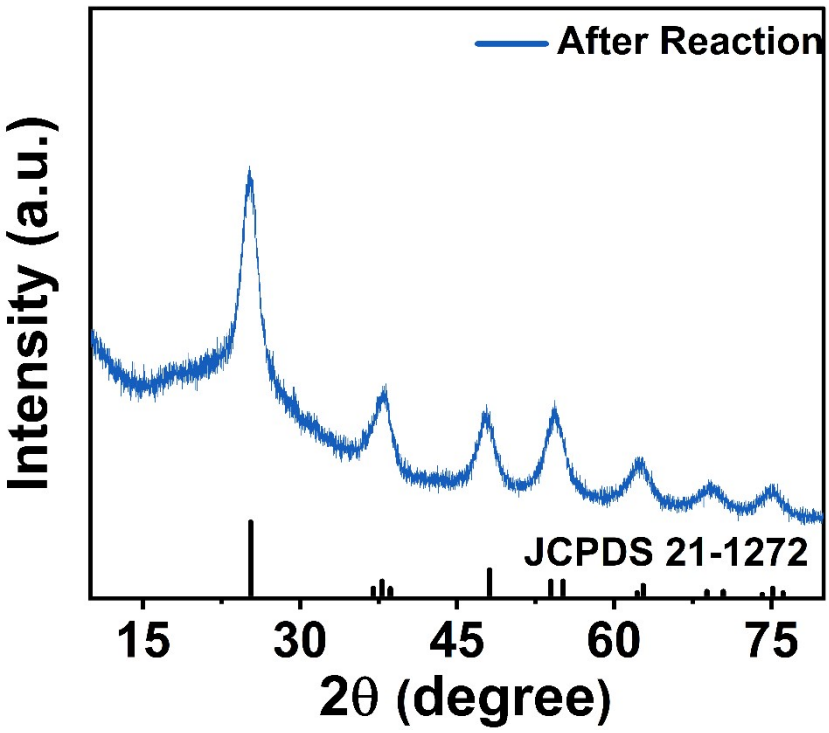

Fig. S16 XRD pattern of W-doped TiO_2 nanocrystals after photocatalysis reaction.

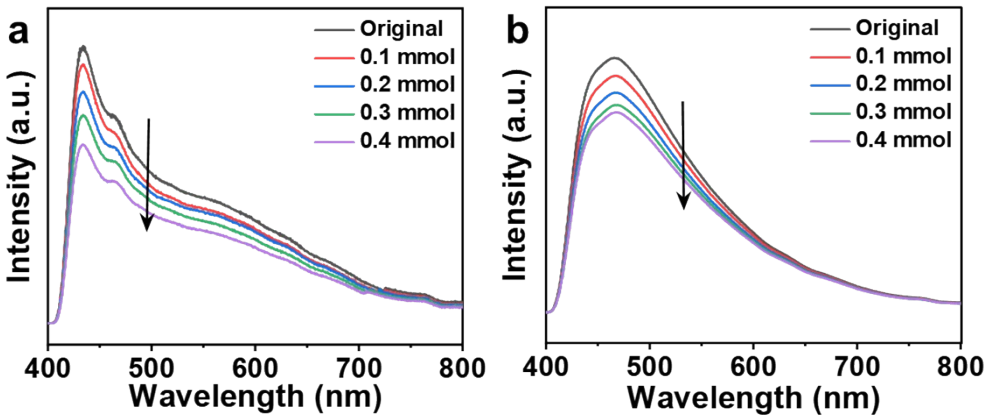

Fig.S17 (a, b) Emission spectra of W-doped TiO_2 (a) and TiO_2 nanocrystals (b) at different concentrations of ethylbenzene.

Table. S1. Parameters of the time-resolved photoluminescence decay curves according to a biexponential decay.

Sample	τ_1	A_1 (%)	τ_2	A_2 (%)	τ_3	A_3 (%)	τ_A
TiO_2	0.1367	18.45	2.1833	29.81	22.6491	51.74	12.41
W-doped TiO_2	0.9614	40.68	6.4199	13.93	59.2489	45.39	28.18

Table. S2. Comparison of the photocatalytic aerobic oxidation of ethylbenzene/toluene activities of the reported heterogeneous materials

Catalyst	Oxidant	Temperature	Substrate（mmol）	Yield (mmol/g)	External filed	Ref.
This work	O_2	rt.	28.3[(a)]	235	435 nm	
CBT	O_2	rt.	8.17[(a)]	14.21	420-780 nm	2
VO@g-C_3N_4	H_2O_2	rt.	1[(a)]	39.62	40 W bulb	3
p-BiOBr	O_2	rt.	0.2[(a)]	9.3	≥420 nm	4
SA-Fe-TCN	O_2	60 °C	0.5[(a)]	9.9	≥420 nm	5
$Cs_3Bi_2Br_9$/SBA-15	Air	rt.	47.16[(a)]	65.8	≥420 nm	6
1.8Ni-BWO	O_2	rt.	21.74[(b)]	45.6	≥420 nm	7
$CsPb_{1-x}Ce_xBr_3$	O_2	rt.	54.34[(b)]	61.2	≥420 nm	8
p-BWO	O_2	rt.	10[(b)]	8.77	≥420 nm	9
$Cs_3Bi_2Br_9$/g-C_3N_4	O_2	rt.	54.34[(b)]	13.59	≥400 nm	10
0.5%Pd@C-GluA-550	Air	120 °C	32.83[(c)]	219.14		11
NCNTs	O_2	120 °C	94.3[(c)]	307.88		12

(a) The substrate of photocatalytic oxidation is ethylbenzene. (b) The substrate of photocatalytic oxidation is toluene. (c) The substrate of thermocatalytic oxidation is ethylbenzene.

References:

1 H. Lin, K. Zhang, G. Yang, Y. Li, X. Liu, K. Chang, Y. Xuan and J. Ye, Ultrafine nano 1T-MoS_2 monolayers with NiO_x as dual co-catalysts over TiO_2 photoharvester for efficient photocatalytic hydrogen evolution, *Appl. Catal. B: Environ.*, 2020, **279**, 119387.

2 R. Yuan, S. Fan, H. Zhou, Z. Ding, S. Lin, Z. Li, C. Xu, L. Wu, X. Wang and X. Fu, Chlorine-Radical-Mediated Photocatalytic Activation of C-H Bonds with Visible Light, *Angew. Chem. Int. Ed.*, 2012, **52**, 1035-1039.

3 S. Verma, R. B. Nasir Baig, M. N. Nadagouda and R. S. Varma, Photocatalytic C-H Activation of Hydrocarbons over VO@g-C_3N_4, *ACS Sustainable Chem. Eng.*, 2016, **4**, 2333-2336.

4 X. Cao, A. Huang, C. Liang, H.-C. Chen, T. Han, R. Lin, Q. Peng, Z. Zhuang, R. Shen, H. Chen, Y. Yu, C. Chen and Y. Li, Engineering Lattice Disorder on a Photocatalyst: Photochromic BiOBr Nanosheets Enhance Activation of Aromatic C-H Bonds via Water Oxidation, *J. Am. Chem. Soc.*, 2022, **144**, 3386-3397.

5 X. Xiao, Z. Ruan, Q. Li, L. Zhang, H. Meng, Q. Zhang, H. Bao, B. Jiang, J. Zhou, C. Guo, X. Wang and H. Fu, A Unique Fe-N_4 Coordination System Enabling Transformation of Oxygen into Superoxide for Photocatalytic C-H Activation with High Efficiency and Selectivity, *Adv. Mater.*, 2022, **34**, 2200612.

6 Y. Dai, C. Poidevin, C. Ochoa-Hernµndez, A. A. Auer and H. Tüysüz, A Supported Bismuth Halide Perovskite Photocatalyst for Selective Aliphatic and Aromatic C-H Bond Activation, *Angew. Chem. Int. Ed.*, 2020, **59**, 5788-5796.

7 Y. Shi, P. Li, H. Chen, Z. Wang, Y. Song, Y. Tang, S. Lin, Z. Yu, L. Wu, J. C. Yu and X. Fu, Photocatalytic Toluene Oxidation with Nickel-mediated Cascaded Active Units over Ni/Bi_2WO_6 Monolayers, *Nat. Commun.*, 2024, **15**, 4641.

8 T. Wang, Y. Li, X. Yang, Y. Hu, X. Du, M. Zhang, Z. Huang, S. Liu, Y. Wang and W. Xie, Efficient C(sp^3)-H Bond Oxidation on Perovskite Quantum Dots Based on Ce-oxygen Affinity, *Angew. Chem. Int. Ed.*, 2024, **63**, e202409656.

9 X. Cao, Z. Chen, R. Lin, W.-C. Cheong, S. Liu, J. Zhang, Q. Peng, C. Chen, T. Han, X. Tong, Y. Wang, R. Shen, W. Zhu, D. Wang and Y. Li, A photochromic composite with enhanced carrier separation for the photocatalytic activation of benzylic C-H bonds in toluene, *Nat. Catal.*, 2018, **1**, 704-710.

10 Z. Bai, Y. Mao, B. Wang, L. Chen, S. Tian, B. Hu, Y.-J. Li, C. Au and S. Yin, Tuning Photocatalytic Performance of $Cs_3Bi_2Br_9$ Perovskite by g-C_3N_4 for C(sp^3)-H Bond Activation, *Nano Res.*, 2022, **16**, 6104-6112.

11 Y. G. Pengfei Zhang, Haoran Li, Zhirong Chen and Yong Wang, Solvent-free aerobic oxidation of hydrocarbons and alcohols with Pd@N-doped carbon from glucose, *Nat. Commun.*, 2013, **4**, 1593.

12 Y. Su, Y. Li, Z. Chen, J. Huang, H. Wang, H. Yu, Y. Cao and F. Peng, New Understanding of Selective Aerobic Oxidation of Ethylbenzene Catalyzed by Nitrogen-doped Carbon Nanotubes, *ChemCatChem*, 2020, **13**, 646-655.